ELSEVIER

Thermochimica Acta 282/283 (1996) 131–142

thermochimica acta

Crystallization kinetics of amorphous RuO_2 [1]

Jiří Málek *, Akio Watanabe, Takefumi Mitsuhashi

National Institute for Research in Inorganic Materials, Namiki 1–1, Tsukuba, Ibaraki 305, Japan

Abstract

The crystallization kinetics of nanocrystalline t-RuO_2 in amorphous ruthenium oxide was studied by differential scanning calorimetry (DSC). It is shown that this process cannot be described by the Johnson–Mehl–Avrami model and that the two-parameter empirical Šesták–Berggren equation gives a more quantitative description. The reliability of kinetic parameters calculated from nonisothermal DSC data is tested by comparing calculated and experimental isothermal data. It is shown that a very good prediction of isothermal behavior can be obtained.

Keywords: Amorphous rutherium oxide; Crystallization kinetics; DSC; Johnson–Mehl–Avrami model; t-RuO_2; Šesták–Berggren model

1. Introduction

For the preparation of nanocrystalline oxides from amorphous precursors it is very important to determine reliable kinetic parameters enabling control of the crystallization process under defined conditions. However, the mathematical description of such complex processes involving both nucleation and crystal growth is not a simple task. The use of phenomenological models based on a formal description of geometrically well defined bodies under strictly isothermal conditions often cannot give a satisfactory result. In this respect, it seems that empirical kinetic models containing the smallest possible number of constants could provide enough flexibility to describe the real process as closely as possible. The kinetic parameters determined from non-isothermal data then can be used for control of the crystal growth under isothermal conditions.

* Corresponding author. Fax: + 42 40 48 400; e-mail: malek@pol.upce.cz. Correspondance address: Joint Laboratory of Solid State Chemistry, Academy of Sciences of the Czech Republic & University of Pardubice, Studentská 84, Pardubice 530 09, Czech Republic.

[1] Dedicated to Takeo Ozawa on the Occasion of his 65th Birthday.

PII: S0040-6031(96)02887-0

The aim of this work is to demonstrate such a possibility for the crystallization of amorphous RuO_2

2. Kinetic model

It is assumed that the heat flow, ϕ, generated during the crystallization process is directly proportional to the rate of crystallization ($d\alpha/dt$):

$$\phi = \Delta H\left(\frac{d\alpha}{dt}\right) \tag{1}$$

where ΔH is the enthalpy of the crystallization process. Assuming the Arrhenius temperature-dependence of the rate constant $K = A\exp(-E/RT)$ the kinetic equation can then be expressed in the form [1]:

$$\phi = \Delta H A\exp(-E/RT)f(\alpha) \tag{2}$$

where A is the pre-exponential factor, E is the activation energy and α is the fractional conversion. The kinetic model function $f(\alpha)$ is derived on the basis of physico–geometric assumptions on the movement of the interface between amorphous solid and newly formed crystalline phase.

The theoretical basis for description of the isothermal crystallization of undercooled liquids and amorphous solids involving both nucleation and growth was formulated by Volmer and Weber [2], Johnson and Mehl [3], Avrami [4–6], and Kolmogorov [7]. A very good review of this topic has been given by Christian [8]. In its basic form, the theory describes the time-dependence of the fractional extent of crystallization, α. The resulting equation is known as the Johnson–Mehl–Avrami (JMA) equation, which can be written in the form:

$$[-\ln(1-\alpha)]^{1/n} = Kt \tag{3}$$

where n is so called Avrami exponent. For some simple cases of crystallization it is possible to find a characteristic value of this kinetic exponent n [8]. By differentiation of Eq. (3) with respect to time and comparing with Eqs. (1) and (2) the $f(\alpha)$ function corresponding to the JMA model can be written as follows:

$$f(\alpha) = n(1-\alpha)[-\ln(1-\alpha)]^{1-1/n} \tag{4}$$

Strictly speaking this equation is valid under isothermal conditions only. However, it has been shown by Ozawa [9, 10] that the validity of the fundamental Eq. (3) can be extended under certain circumstances for nonisothermal conditions also. Two simple models for the case of crystal growth from preexisting nuclei with negligible concurrent random nucleation were proposed [9, 10]. The first model is that of crystal growth from a nucleating agent where the number of nuclei is independent of the thermal history of the material. The second model refers to the situation where the temperature range for random nucleation is clearly separated from that for crystal growth. In this case the

number of nuclei is constant during crystal growth but dependent on the thermal history in the nucleation temperature range. Similar conclusions were drawn also by Henderson [11, 12] and also by DeBruijn et al. [13]. Therefore, the validity of the JMA model, as defined by Eq. (4), can be extended to nonisothermal conditions if the following two conditions are fulfilled:

(1) homogeneous nucleation or heterogeneous nucleation at randomly dispersed second phase particles; and
(2) the growth rate of new phase is controlled by temperature and is independent of time.

Nevertheless, the applicability of the JMA model should be considered very carefully even when both these conditions are valid. Recently, Shepilov and Baik [14] have demonstrated that for highly anisotropic crystal growth the JMA approximation may no longer be valid.

It is evident that the applicability of the JMA kinetic model should be tested before any quantitative analysis of experimental data is made. Recently, such testing methods were proposed [15] on the basis of the $z(\alpha)$ function defined as follows:

$$z(\alpha) = \phi T^2 \tag{5}$$

The $z(\alpha)$ function can, therefore, be easily obtained by very simple transformation of the experimental DSC data just by multiplying measured heat flow by T^2. This can be done without needing to know any kinetic parameter. It can be shown [15] that for the JMA model the position of the maximum of the $z(\alpha)$ function should be $\alpha_p^\infty = 0.632$. An important fact is that this value of α_p^∞ does not depend on kinetic parameters E and A, or on the kinetic exponent n for the JMA model. In fact these values depend slightly on procedural parameters, e.g. heating rate, the thermal conductivity of the DSC cell and the heat capacity of sample, thermal inertia effects, etc. Nevetheless, the deviation from the value $\alpha_p^\infty = 0.632$ should not exceed 3% in the case of the JMA model. Using this method it is possible to verify the applicability of the JMA model even using one DSC curve only. It is convenient, however, to compare $z(\alpha)$ functions for several DSC measurements taken at different heating rates. If normalized plots have identical shapes with a maximum within the range specified above then TA data can be probably described within the JMA model.

If the maximum of the $z(\alpha)$ function is $\alpha_p^\infty < 0.632$ then one (or more) of the aforementioned conditions is not fulfilled and the JMA model cannot be used for description of the experimental data. Usually, it is because of overlapping of nucleation and crystal growth processes with the result that the site saturation condition is no longer held. As a consequence the maximum of the $z(\alpha)$ function will differ from its theoretical value for the JMA model. In this case, it is convenient to use more flexible empirical kinetic model functions, $f(\alpha)$, for the description of crystallization process, e.g. the Šesták–Berggren (SB) empirical kinetic model [16]:

$$f(\alpha) = \alpha^M (1-\alpha)^N \tag{6}$$

This flexible two-parameter SB function, in fact, also includes the JMA model. It can be shown [17] (see Fig. 4) that there are combinations of parameters M and N corre-

sponding to a given value of kinetic exponent for the JMA model ($n \geq 1$). Therefore, the SB kinetic model can be used for a quantitative description of more complex crystallization processes involving partially overlapping nucleation and growth phases. The kinetic exponent, M and N in Eq. (6), are characteristic of a particular crystallization process although it is rather problematic to find their real physical meaning. It was shown [18], however, that physically meaningful values of the parameter M should be confined in the range: $0 < M < 1$.

The kinetic exponents of the JMA or SB model as well as the Arrhenius parameters E and $\ln A$ in Eq. (2) can be calculated using a method described previously [17]. These kinetic parameters, obtained for nonisothermal conditions, can be used for the construction of Time–Temperature–Transformation (TTT) diagrams in order to predict the behavior of the system under isothermal conditions. For such predictions we can use the following equation obtained by integration of Eqs. (1) and (2) under isothermal conditions:

$$t = \frac{\exp(E/RT)}{A} \int_0^{\alpha} \frac{d\alpha}{f(\alpha)} \tag{7}$$

The integral in Eq. (7) can be expressed analytically for the JMA model—$[-\ln(1-\alpha)]^{-1/n}$—but it has to be calculated numerically for the SB model.

3. Experimental

The sample of amorphous RuO_2 was prepared from $RuCl_3$ (Furuya Kinzoku, metallic impurities $< 0.25\%$) dissolved in 1 N hydrochloric acid. By addition of 2 N NH_4OH to this solution the black hydroxide $Ru(OH)_3$ was precipitated ($pH \approx 3.0$–5.5). The precipitated gel was washed three times in distilled water to remove chloride ions, filtered, and dried in air at 100°C for 10 h. The ruthenium(III) hydroxide was very unstable, being oxidized by air to $RuO_2 \cdot nH_2O$ during this treatment. This product is denoted here *as prepared* sample and it was subjected to crystallization studies as described in following section.

Differential scanning calorimetry (DSC) measurements of the crystallization kinetics were performed by using a Perkin–Elmer Model DSC-7 on samples of about 10 mg encapsulated in aluminum sample pans in an atmosphere of dry nitrogen. The instrument was previously calibrated with In, Pb, and Zn standards. Nonisothermal DSC curves were obtained with selected heating rates 2–20 K min^{-1} in the range 25–600°C. Kinetic analysis of the DSC data was performed by the TA–System software package [17]. Thermogravimetric experiments were carried out in an atmosphere of dry nitrogen using a Perkin–Elmer Model TGA-7.

RuO_2 phase identification was performed using a Rigaku Model RINT2000 X-ray diffractometer (XRD) equipped with horizontal goniometer and scintillation counter, utilizing Ni-filtered CuK_α radiation (40 kV, 30 mA). The scans were made over a 2θ range of 50–100° at the slow scanning speed of 0.6° 2θ min^{-1}. The morphology of as prepared and partially crystallized samples was examined by scanning electron microscopy (SEM) using a Hitachi Model S-5000 microscope.

4. Results and discussion

The 'as prepared' sample of hydrated ruthenium oxide continuously loses water when heated, as is demonstrated in Fig. 1. The crystallization process starts when nearly all the water has been removed from the sample; water loss during the crystallization is less than 1.2%. The slope of DSC curve before and after the crystallization process is different, and the difference increases with the heating rate. Such behavior is probably caused by shrinking of the sample connected with water removal as well as by the different thermal conductivities of the crystallized amorphous samples. The crystallization enthalpy of as prepared sample was found to be $-\Delta H_c = 175 \pm 5\ J\ g^{-1}$. During isothermal treatment of 'as received' RuO_2 at various temperatures above 300°C crystallization takes place. In this way several partially crystallized RuO_2 samples were prepared. The conditions of preparation are shown in Table 1. The degree of crystallization α_c can be estimated from the crystallization enthalpy ΔH_c determined from the nonisothermal DSC run performed after previous cooling of partially crystallized samples.

Fig. 2 shows the results of a typical kinetic analysis of crystallization data corresponding to sample A. Experimental data (points) for different heating rates are compared with DSC curves calculated for the SB model (full lines). The $z(\alpha)$ functions calculated using Eq. (5) are shown in the inset. The maximum of the $z(\alpha)$ function is considerably lower than the characteristic α_p^∞ value for the JMA model. A similar result was also obtained for samples B–E. The maximum of the $z(\alpha)$ function changes only

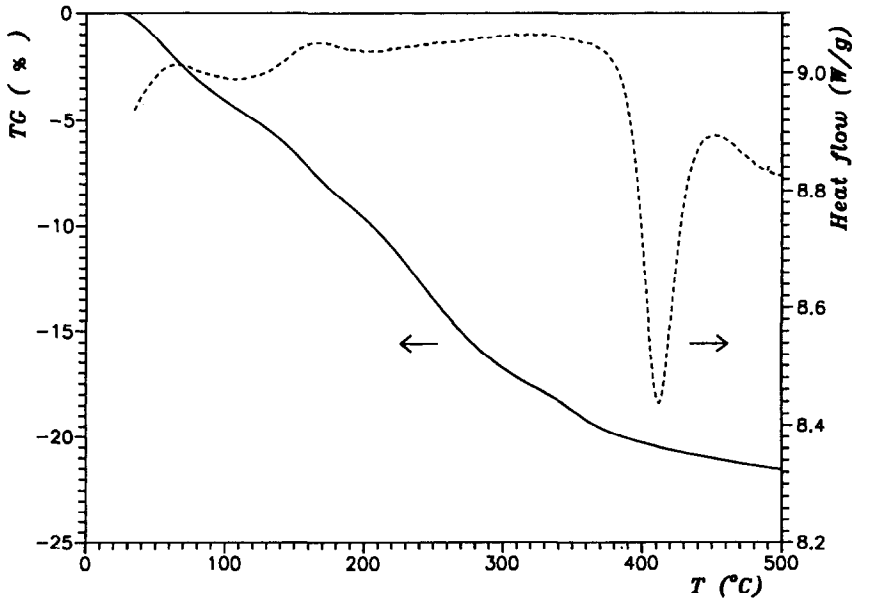

Fig. 1. Typical TG (full line) and DSC (broken line) curves of 'as prepared' sample A measured with nitrogen gas flow at 5 K min^{-1}.

Table 1
Preparation and characterization of RuO_2 samples

Sample	Method of preparation	$-\Delta H_c/(J\ g^{-1})$	α_c
A	'As prepared' sample	175±5	0
B	Treatment at 310°C for 1 h	149±5	0.15±0.03
C	Treatment at 340°C for 1 h	135±7	0.23±0.04
D	Treatment at 350°C for 1 h	99±7	0.43±0.05
E	Treatment at 360°C for 1 h	61±4	0.65±0.06
F	Heating at 10 K min^{-1} up to 600°C	–	1

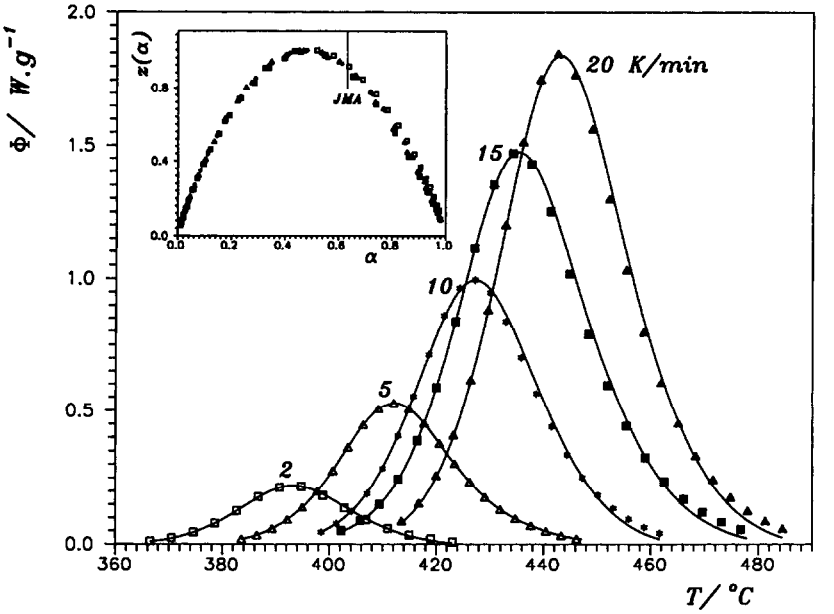

Fig. 2. Experimental DSC curves for sample A (points) measured with nitrogen gas flow at heating rates of 2–20 K min^{-1}. Full lines were calculated for the SB model using kinetic parameters shown in Table 2. Inset shows the $z(\alpha)$ dependences calculated from DSC data using Eq. (5). The α_p^x value typical for the JMA model is marked with a line.

slightly with the fraction crystallized and it is far from the value predicted for the JMA model, as is illustrated in Fig. 3. It seems that one or more conditions for the applicability of the JMA equation is not fulfilled and that the two-parameter SB model should be used in this case. The kinetic parameters calculated for this model are summarized in Table 2.

The variation of the activation energy value does not exceed 10%, which is usually considered to be within experimental error. The kinetic exponent N is also practically independent of the fraction crystallized. On the other hand the exponent M changes

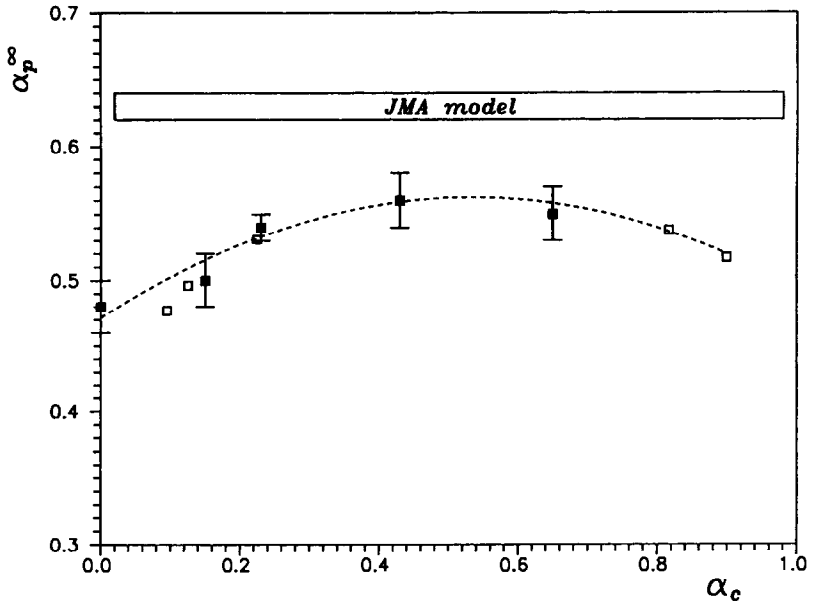

Fig. 3. The α_p^∞ value as a function of the fraction crystallized, α_c, for the samples A–E (points). The broken line is drawn as a visual guide. Full lines represent the limits of applicability of the JMA model.

Table 2
Kinetic parameters for crystallization of amorphous and partially crystalline RuO_2 samples

Sample	M	N	E/(kJ mol^{-1})	ln[A/s^{-1}]	α_p^∞
A	0.63±0.02	1.31±0.06	168±3	25.0±0.1	0.48±0.02
B	0.53±0.04	1.28±0.09	179±7	27.2±0.1	0.50±0.02
C	0.38±0.02	1.30±0.03	185±6	28.1±0.1	0.54±0.01
D	0.21±0.03	1.31±0.03	195±2	29.9±0.2	0.56±0.02
E	0.18±0.04	1.22±0.04	181±5	27.2±0.1	0.55±0.02

substantially with the degree of crystallization. Fig. 4 illustrates this behavior in the M–N plane where theoretical prediction for the JMA model is also shown. Again, it is seen that our data do not match the prediction for the JMA model. Unfortunately, there is no direct link between the values of the kinetic exponents of the SB model and the real mechanism of the crystallization process. Therefore it is rather difficult to quantify the departure of our data from the JMA model and the kinetic exponents M and N should be understood rather as numerical constants describing overall crystallization process.

The kinetic parameters calculated using non-isothermal DSC data can be used to control the crystallization process under isothermal conditions. This is shown in Fig. 5

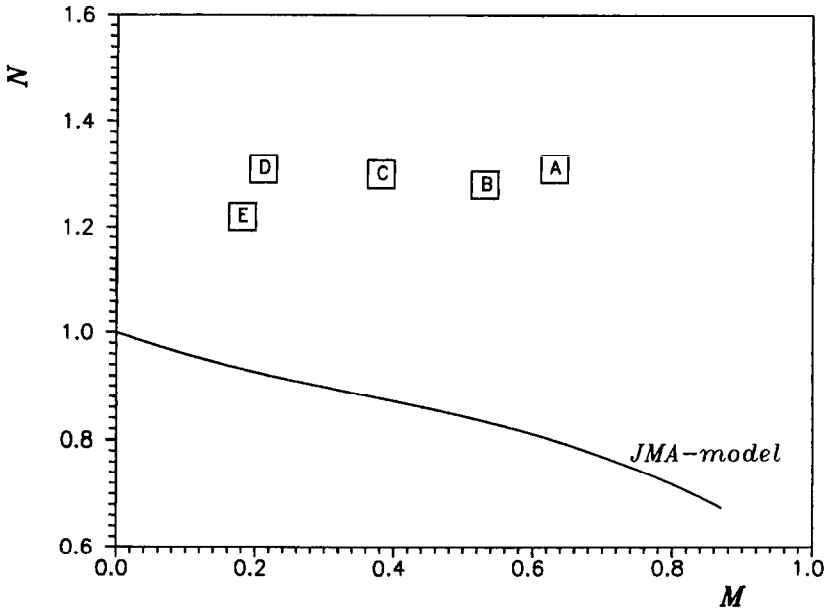

Fig. 4. M–N diagram for the SB model. The combinations of kinetic exponents corresponding to the JMA model are shown by the full line. Points correspond to kinetic parameters for the samples A–E.

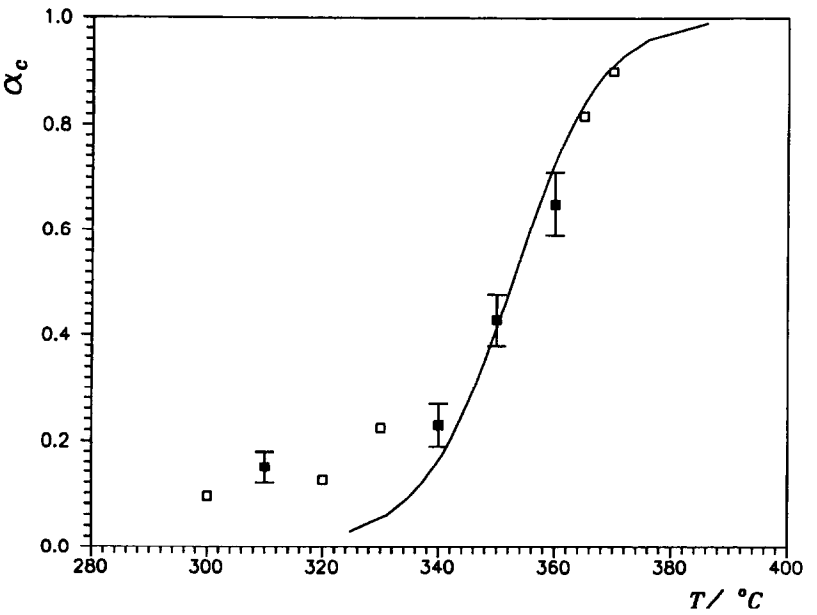

Fig. 5. The fraction crystallized, as a function of temperature, after 1-h treatment of amorphous RuO_2. Experimental data are shown by points: (■) samples B–E, (□) other measurements. The curve was calculated using Eq. (8) for the SB model using the kinetic parameters for the 'as prepared' sample A (Table 2).

where experimental data and the expected temperature-dependence of the degree of crystallization are compared. Direct isothermal measurement of the crystallization kinetics of amorphous RuO_2 is problematic because the exothermic effect due to the crystallization overlaps with endothermic effect corresponding to the release of water retained in the sample, thus reducing the accuracy of the results. Thus, in this case the residual enthalpy of crystallization (ΔH_R) was measured using samples scanned at 10 K min^{-1} after isothermal treatment in a DSC calorimeter. The fraction crystallized, α_c, can be estimated using the equation $\alpha_c = (\Delta H_c - \Delta H_R)/\Delta H_c$, where ΔH_c is the enthalpy of crystallization of the 'as prepared' sample. The points in Fig. 5 correspond to isothermal crystallization after treatment for 1 h at different temperatures and the curves were calculated using Eq. (8) for kinetic parameters corresponding to the 'as prepared' sample A. It is seen that except for the temperatures below 340°C there is quite good agreement between isothermal experimental data and the curves calculated using kinetic parameters obtained from nonisothermal measurement. Fig. 6 shows the isothermal dependence of the fraction of amorphous RuO_2 crystallized at 340°C. Above this temperature the empirical SB model can be used satisfactorily for description of the process of crystallization of amorphous RuO_2.

Room temperature XRD patterns for the 'as received' sample (A) and fully crystallized sample (F) are shown in Fig. 7. Sample A exhibits an XRD pattern typical of an amorphous sample. The XRD pattern for the fully crystallized sample corresponds to

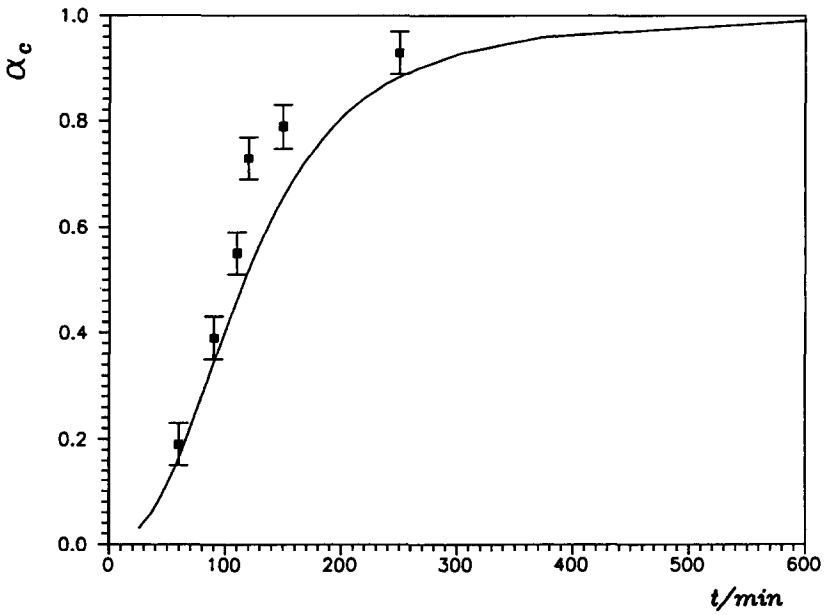

Fig. 6. Isothermal dependence of the crystallized fraction of amorphous RuO_2 at 340°C. Experimental data are shown by points. The curve was calculated using Eq. (8) for the SB model using the kinetic parameters for sample A (Table 2).

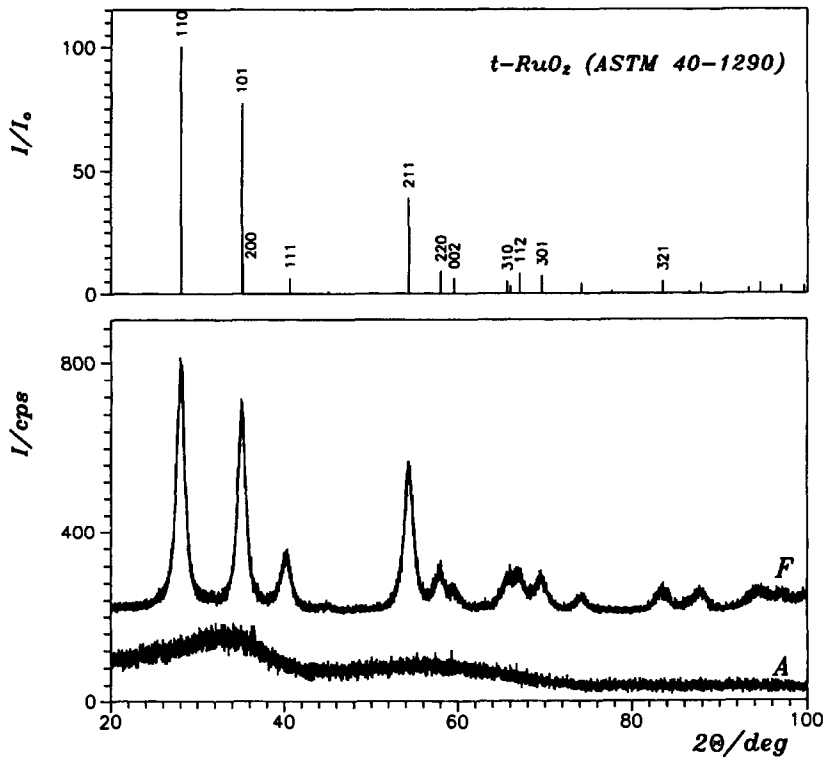

Fig. 7. XRD pattern for amorphous and fully crystallized RuO_2 (samples A and F). The bar diagram corresponds to the ASTM data for tetragonal RuO_2.

a tetragonal RuO_2 phase. The calculated lattice parameters ($a = 0.4499 \pm 0.0002$ nm, $c = 0.3108 \pm 0.0002$ nm) agree well with published ASTM data. The apparent crystallite size estimated from the diffraction peak-width at half-maximum intensity of the tetragonal (110) peak was found to be about 10 nm. This is slightly smaller than is directly observed by SEM. A typical SEM micrograph is shown in Fig. 8, which shows the typical size of RuO_2 crystals to be between 15 and 30 nm.

5. Conclusion

The kinetic analysis of the process of crystallization of nanocrystalline tetragonal RuO_2 in amorphous ruthenium oxide is presented. Nonisothermal measurements at various heating rates enable calculation of kinetic parameters characterizing the crystallization process. A very simple and convenient method enables assessment of the applicability of the Johnson–Mehl–Avrami model. It was found, however, that the process of crystallization of amorphous RuO_2 cannot be described successfully by this

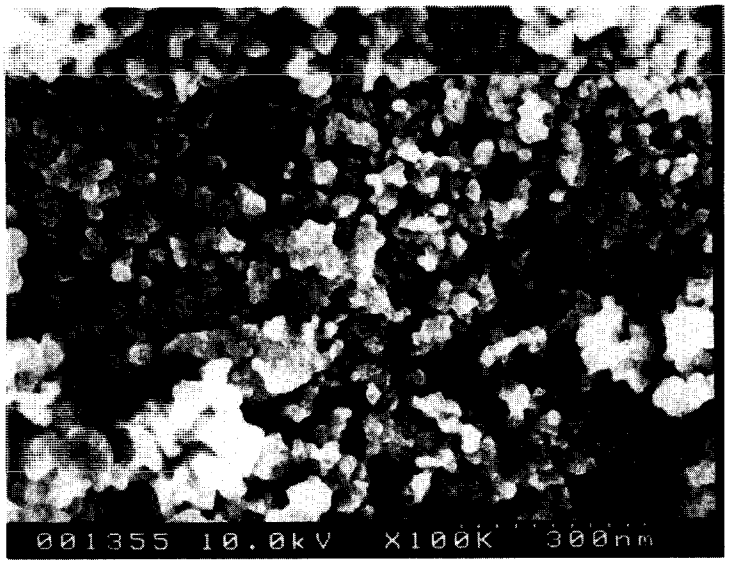

Fig. 8. SEM micrograph of fully crystallized RuO_2 (sample H).

model and that the two-parameter Šesták–Berggren equation seems to be more appropriate in this case.

The kinetic parameters calculated from kinetic analysis of nonisothermal DSC data can be used for the prediction of the crystallization kinetics under isothermal conditions, as is demonstrated by comparison of experimental and calculated isothermal crystallization curves.

Acknowledgments

This work is partially supported by the Cross-over research project on underlying technology of nuclear energy, promoted by the Science and Technology Agency of Japan (STA). One of the authors (JM) is grateful to the STA for financial support within the STA Fellowship Program. The authors are indebted to Mr. M. Tsutsumi for his valuable help with SEM observations.

References

[1] J. Šesták, Thermophysical Properties of Solids, Their Measurements and Theoretical Analysis, Elsevier, Amsterdam, 1984.
[2] M. Volmer and A. Weber, Z. Phys. Chem., 119 (1926) 227.
[3] W.A. Johnson and R.F. Mehl, Trans. Am. Inst. Min. (Metall.) Engs., 135 (1939) 416.
[4] M. Avrami, J. Phys. Chem., 7 (1939) 1103.
[5] M. Avrami, J. Phys. Chem., 8 (1940) 212.

[6] M. Avrami, J. Phys. Chem., 9 (1941) 177.
[7] A.N. Kolmogorov, Izvestia Akad. Nauk USSR, Ser. Math. 1 (1937) 355.
[8] J.W. Christian, The Theory of Transformations in Metals and Alloys, Pergamon, New York, 2nd ed 1975.
[9] T. Ozawa, Polymer, 12 (1971) 150.
[10] T. Ozawa, Bull. Chem. Soc. Jpn., 57 (1984) 639.
[11] D.W. Henderson, J. Therm. Anal., 15 (1979) 325.
[12] D.W. Henderson, J. Non-Cryst. Solids, 30 (1979) 301.
[13] T.J.W. DeBruijn, W.A. DeJong and P.J. Van Den Berg, Thermochim. Acta, 45 (1981) 315.
[14] M.P. Shepilov and D.S. Baik, J. Non-Cryst. Solids, 171 (1994) 141.
[15] J. Málek, Thermochim. Acta, 267 (1995) 61.
[16] J. Šesták and G. Berggren, Thermochim. Acta, 3 (1971) 1.
[17] J. Málek, Thermochim. Acta, 200 (1992) 257.
[18] J. Málek, J.M. Criado, J. Šesták and J. Militký, Thermochim. Acta, 153 (1989) 429.